Supporting Information

Tatituri et al. 10.1073/pnas.1220601110

SI Materials and Methods

Mice. C57BL/6 mice were obtained from Jackson Laboratory. MyD88$^{-/-}$ mice were provided by K. Kobayashi (Harvard Medical School, Boston). All mice were housed in specific pathogen-free conditions, and female mice at 6–14 wk of age were used for experiments. All animal studies were approved by the Dana-Farber Cancer Institute Animal Care and Use Committee.

In Vitro NKT Cell Assays and *Mtb* Infection. The CD1d-restricted T-cell hybridomas 14S.6, TBA7, VII68, 14S.10, 431.A11, 14S.15, XV19, and VIII24 (dNKT cell) and 24.9 (iNKT cell) were described (1–3) and maintained in complete RPMI medium [RPMI supplemented with 10% (vol/vol) FBS (Gemini), Hepes, L-glutamine, penicillin/streptomycin, and 2-mercaptoethanol (Invitrogen)]. RAW.267 cells transfected with mouse CD1d were maintained in complete DMEM and used in coculture experiments. Murine iNKT cell lines and BMDCs were generated as described (4). Hybridomas or iNKT cell lines (1×10^5 to 2×10^5 per well) were cultured with RAW cells or BMDCs (10^4 to 10^5 per well) in 96-well plates (Costar; Corning) in complete RPMI. Microbial lipids or stimuli were added, and cultures were incubated for 16–48 h at 37 °C. For infection experiments, *Mtb* H37Rv was prepared and added to RAW cells at various multiplicities of infection (MOIs) as described (5). Hybridoma lines were added to the infected RAW cells immediately following infection with *Mtb* and cocultured for 24 h. MOI was determined by taking a ratio of bacterial burden, based on CFU measurements, to macrophage number. Culture supernatants were analyzed by ELISA with matched antibody pairs for IL-2 or IFN-γ (BD Pharmingen). For fix→pulse/pulse→fix experiments, RAW.CD1d cells were fixed with 0.04% paraformaldehyde for 10 min before or after loading with antigen and coculture assays with hybridoma cells were performed as described above.

Determination of TCR α- and β-Chain Sequences of NKT Hybridomas. mRNA from hybridomas was extracted by using TRIzol (Invitrogen) and reverse-transcribed into cDNA by using a cDNA synthesis kit (Qiagen) following manufacturer's instructions. Vα, Vβ, Cα, and Cβ primers and PCR conditions have been described (6). PCR products were sequenced, and TCR-α and -β gene use was analyzed by using the International ImMunoGeneTics Information System database (www.imgt.org).

Bacteria and Isolation of Microbial Lipids. Lyophilized γ-irradiated *Mtb* and *Mtb* whole-cell lysates were provided by Colorado State University (Fort Collins, CO). *Cg* was grown in LB culture medium at 37 °C until mid- to late-log phase and washed ×3 with PBS. Bacteria were lyophilized, and lipids were extracted and analyzed by TLC as described (7) or analyzed by HPLC using an AutoPurification HPLC system coupled to a mass detector with both electrospray (ES) and atmospheric pressure chemical ionization capabilities, evaporative light scattering detector, and photodiode array detector (Waters) (4). Glycolipids were visualized by spraying TLC plates with α-naphthol/sulfuric acid followed by gentle charring of plates, by spraying with 5% ethanolic molybdophosphoric acid and charring, or by using a Dittmer and Lester reagent that is specific for phospholipids and glycophospholipids.

Lipids. Synthesis of 16:0/18:1 and 18:1/16:0 PG will be described elsewhere. All other lipids were from Avanti Polar Lipids.

Generation of pgsA-Deficient *Cg*. To enable the specific deletion of NCgl1889, the gene encoding for pgsA (Fig. S4), in the chromosome of WT *Cg* the nonreplicative plasmid pK19mobsacBΔ1889 was constructed (8). By using primer pairs P1 (CGTTCCCGGG CTCGCGGTGGACGGTACGAAC) and P2rev (CCCATCCACTAAACTTAAACAGGTGTTCCACCCTACCTGCACCC) the 3′ end of the gene was amplified, and using primer pairs P3 (TGTTTAAGTTTAGTGGATGGGTACCTGTGGGATTCACGAAAGTCC) and P4rev (GCTTCCCGGGTTGCCATCGCACGGGCGCACTG) the 5′ end. The resulting fragments served in a cross-over PCR with P1 and P4rev as primers as template to generate a 593-bp fragment containing 12 nt of the 3′ end of NCgl1889 together with genomic upstream sequences and 36 nt of the 5′ end together with genomic downstream sequences. It was cloned via its SmaI sites into pk19mobsacB, and the insert of pK19mobsacBΔ1889 was verified by sequencing. For expression of NCgl1889 the fragment generated by the primer pairs Ex1889RBSfor (GATTATGTCGACAAGGAGATATAGATGTGCAGGTAGGGTGGAACACCG) and Ex1889rev (GATATTGAATTCCTAGCTTTCTGCGGACTTTCGTG) was cloned via SalI and EcoRI sites into pEKEx2 (9), with the insert of pEKEx2-1889 verified by sequencing. Plasmid pK19mobsacBΔ1889 was used to transform *Cg* to kanamycin resistance, indicating chromosomal integration. Sucrose-resistant clones were selected in a second round of positive selection, indicating loss of the vector-encoded sacB function. The specific deletions were verified by PCR. Plasmid pEKEx2-1889 served for complementation studies. Plasmids were introduced in *Cg* by electroporation as described (10). Use of the deletion vector pK19mobsacBΔ1889 and positive selection for integration with subsequent positive selection for loss of vector, yielded 5 mutants out of the 10 clones inspected that had lost chromosomal NCgl1889, whereas in the remaining 5 clones, the WT situation was restored. One of the representative mutants, termed *C. glutamicum* ΔpgsA2, was analyzed in more detail. Growth of the mutant in liquid minimal medium CGXII was only slightly reduced from 0.39 to 0.33 h^{-1}, as was the final optical density. Transformation of *C. glutamicum* ΔpgsA2 with pEKEx2-1889 restored growth ($\mu = 0.41$ h^{-1}).

Structural Analysis of Lipids. MS analysis, including low-energy collisionally activated dissociation multistage MS (MSn) experiments, were conducted on a linear ion-trap mass spectrometer (Finnigan; Thermo Fisher Scientific) with Xcalibur operating system (4, 11). Lipid extracts dissolved in chloroform/methanol (1/2) were continuously infused (2 μL/min) to the ESI source, where the skimmer was set at ground potential, the ES needle was set at 4.5 kV, and temperature of the heated capillary was 300 °C. The automatic gain control of the ion trap was set to 2×10^4, with a maximum injection time of 100 ms. Helium was used as the buffer and collision gas at a pressure of 10−3 mbar (0.75 mTorr). The MSn experiments were performed with an optimized relative collision energy ranging from 18% to 25%, an activation q value at 0.25, and the activation time at 30–50 ms to leave a minimal residual abundance of precursor ion (~10%). Mass spectra were accumulated in the profile mode, typically for 3–10 min for MSn ($n = 2$, 3, and 4) spectra. The mass resolution of the instrument was tuned to 0.6 D at half peak height.

CD1d Binding and Plate Assays. Mouse biotinylated CD1d was from the National Institutes of Health tetramer facility. For loading, lipids were dried under nitrogen, sonicated in 0.05% (vol/vol) Tween-20, and incubated overnight at 37 °C with CD1d. A molar

loading ratio (lipid to CD1d) of 50:1–200:1 was used. For plate-bound CD1d assays, 0.25 μg of loaded CD1d was added to each well of a 96-well streptavidin-coated plate (Thermo Scientific), bound at 25 °C for 30 min, and washed extensively before the addition of iNKT cells. Lipid binding assays were performed as described with small modifications (12). Briefly, CD1d-Fc fusion protein was incubated with di18:1-biotin at a molar ratio of 20:1 overnight, and lipids were added to compete for binding for 4–6 h. CD1d/lipid complexes were then incubated on streptavidin-coated plates (Corning), and bound biotin–lipid/CD1d complexes were detected with anti-Fc Abs and 3,3′,5,5′-tetramethylbenzidine substrate.

1. Cardell S, et al. (1995) CD1-restricted CD4+ T cells in major histocompatibility complex class II-deficient mice. *J Exp Med* 182(4):993–1004.
2. Behar SM, Podrebarac TA, Roy CJ, Wang CR, Brenner MB (1999) Diverse TCRs recognize murine CD1. *J Immunol* 162(1):161–167.
3. Park SH, et al. (2001) The mouse CD1d-restricted repertoire is dominated by a few autoreactive T cell receptor families. *J Exp Med* 193(8):893–904.
4. Brigl M, et al. (2011) Innate and cytokine-driven signals, rather than microbial antigens, dominate in natural killer T cell activation during microbial infection. *J Exp Med* 208(6):1163–1177.
5. Sada-Ovalle I, Chiba A, Gonzales A, Brenner MB, Behar SM (2008) Innate invariant NKT cells recognize Mycobacterium tuberculosis-infected macrophages, produce interferon-gamma, and kill intracellular bacteria. *PLoS Pathog* 4(12):e1000239.
6. Dash P, et al. (2011) Paired analysis of TCRα and TCRβ chains at the single-cell level in mice. *J Clin Invest* 121(1):288–295.
7. Tatituri RV, et al. (2007) Inactivation of Corynebacterium glutamicum NCgl0452 and the role of MgtA in the biosynthesis of a novel mannosylated glycolipid involved in lipomannan biosynthesis. *J Biol Chem* 282(7):4561–4572.
8. Schäfer A, et al. (1994) Small mobilizable multi-purpose cloning vectors derived from the Escherichia coli plasmids pK18 and pK19: selection of defined deletions in the chromosome of Corynebacterium glutamicum. *Gene* 145(1):69–73.
9. Eikmanns BJ, Kleinertz E, Liebl W, Sahm H (1991) A family of Corynebacterium glutamicum/Escherichia coli shuttle vectors for cloning, controlled gene expression, and promoter probing. *Gene* 102(1):93–98.
10. Eggeling L, Bott M (2005) *Handbook of Corynebacterium glutamicum* (CRC/Taylor & Francis, Boca Raton, FL).
11. Hsu FF, Turk J (2010) Toward total structural analysis of cardiolipins: Multiple-stage linear ion-trap mass spectrometry on the [M - 2H + 3Li]+ ions. *J Am Soc Mass Spectrom* 21(11):1863–1869.
12. Rauch J, et al. (2003) Structural features of the acyl chain determine self-phospholipid antigen recognition by a CD1d-restricted invariant NKT (iNKT) cell. *J Biol Chem* 278 (48):47508–47515.

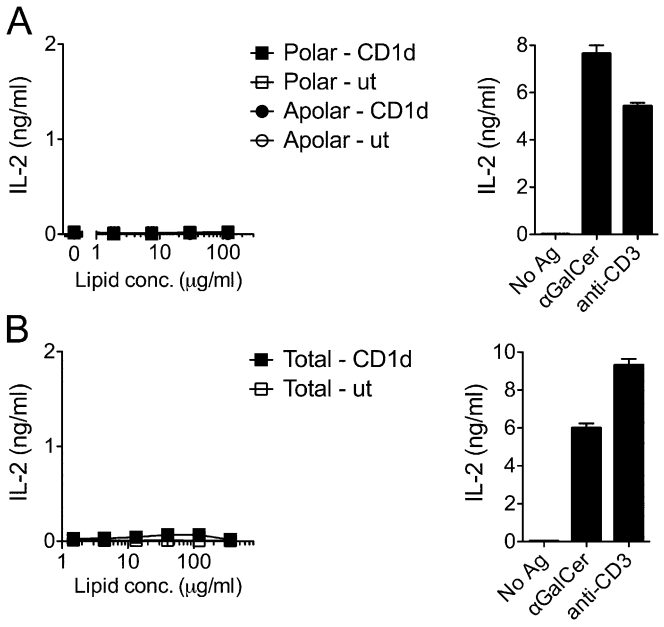

Fig. S1. iNKT cell hybridomas are stimulated by α-GalCer but not by *Mtb* lipids. (*A*) The iNKT cell hybridoma 24.9 was incubated with *Mtb* polar or apolar lipids, and (*B*) the iNKT cell hybridoma DN32 with total *Mtb* lipids, in the presence of RAW.CD1d or RAW.ut cells (*Left*), or with α-GalCer or anti-CD3 antibodies (*Right*).

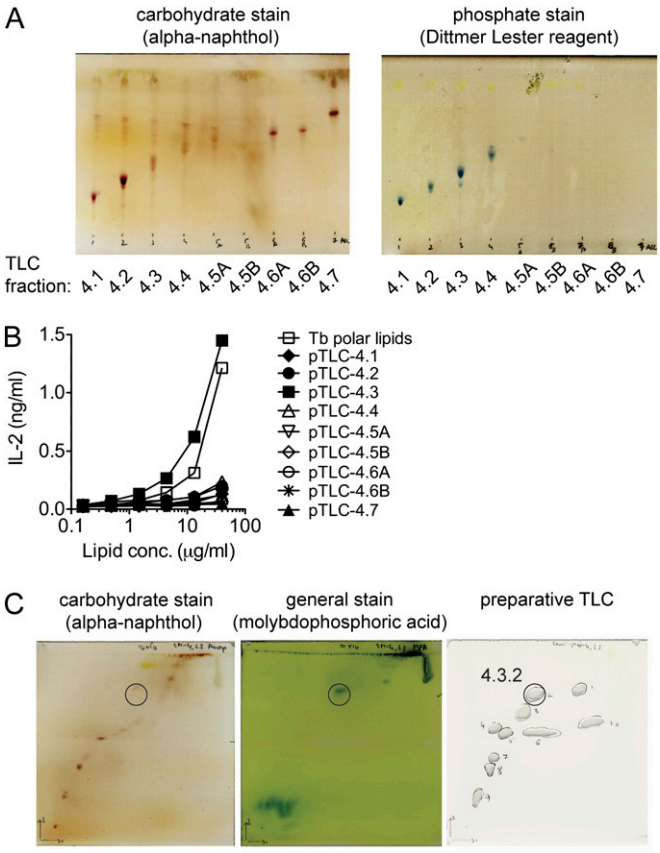

Fig. S2. Purification and isolation of stimulatory *Mtb* lipids. (*A*) Stimulatory *Mtb* polar lipid semiprep 4 was further separated by preparative 1D TLC. Fractions 4.1–7 were analyzed by TLC and stained with α-naphthol (carbohydrate stain; left panel) or with Dittmer Lester reagent (phosphate stain; right panel). (*B*) Fractions 4.1–7 were tested with 14S.10 dNKT hybridoma cells in the presence of RAW.CD1d cells. IL-2 was measured in culture supernatants. (*C*) Stimulatory fraction 4.3 was further separated into 10 lipids by preparative 2D TLC. Circle indicates stimulatory lipid 4.3.2.

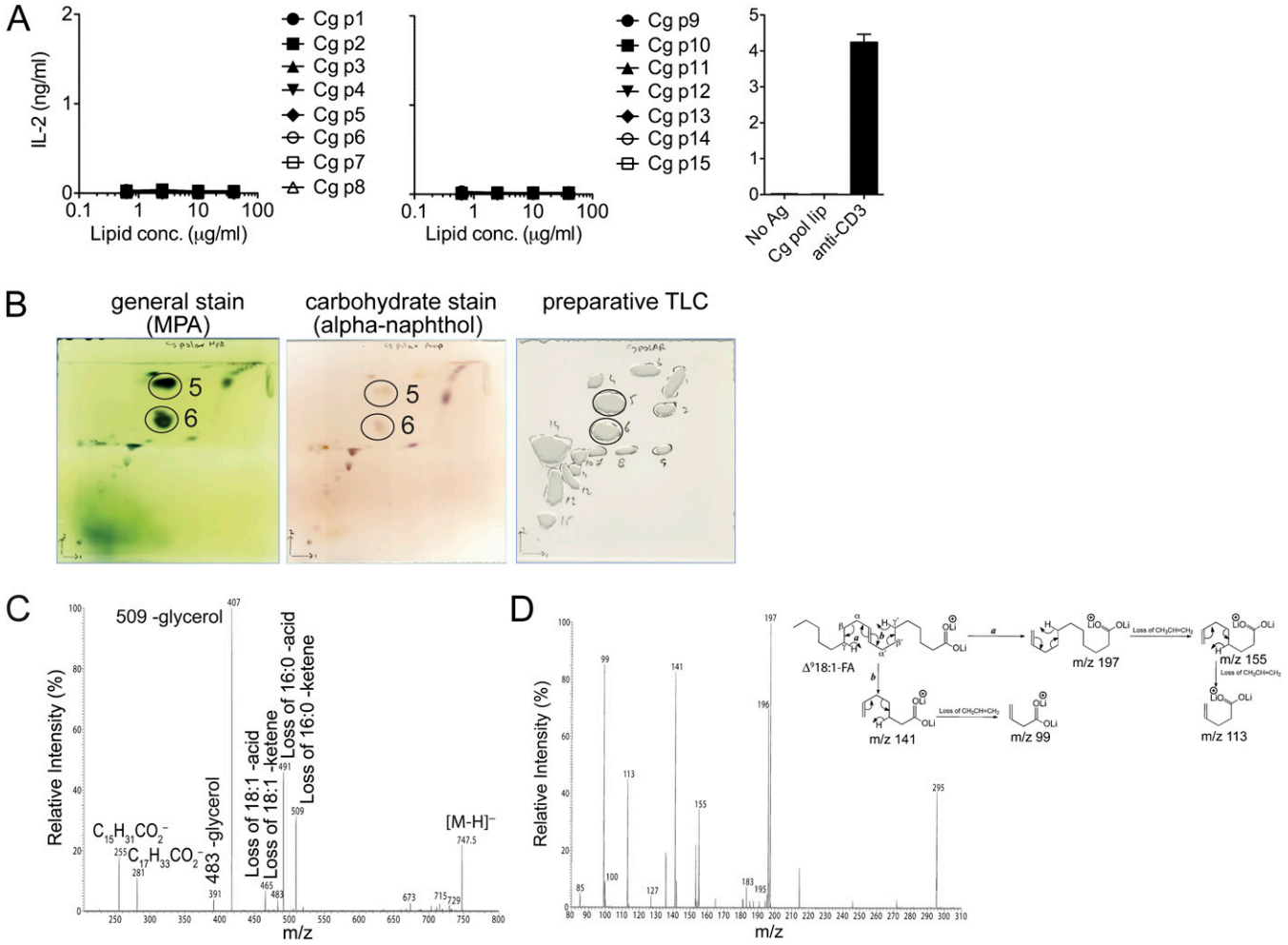

Fig. S3. Structural analysis of stimulatory *Cg* lipids. (*A*) Stimulation of the invariant 24.9 NKT cell hybridoma with *Cg* lipid fractions as in Fig. 3*B*. (*B*) *Cg* lipids were separated by 2D TLC and stained with molybdophosphoric acid (MPA; general lipid stain, left) or α-naphtol (carbohydrate stain, middle), and 15 lipids were isolated by prep-TLC (right, post removal of silica). Stimulatory lipids are marked. (*C*) Collision induced dissociation MS analysis of *Cg* fraction p6 revealed the lipid to be phosphatidylglycerol with several molecular species and (*D*) to contain $\Delta^9$18:1-fatty acid.

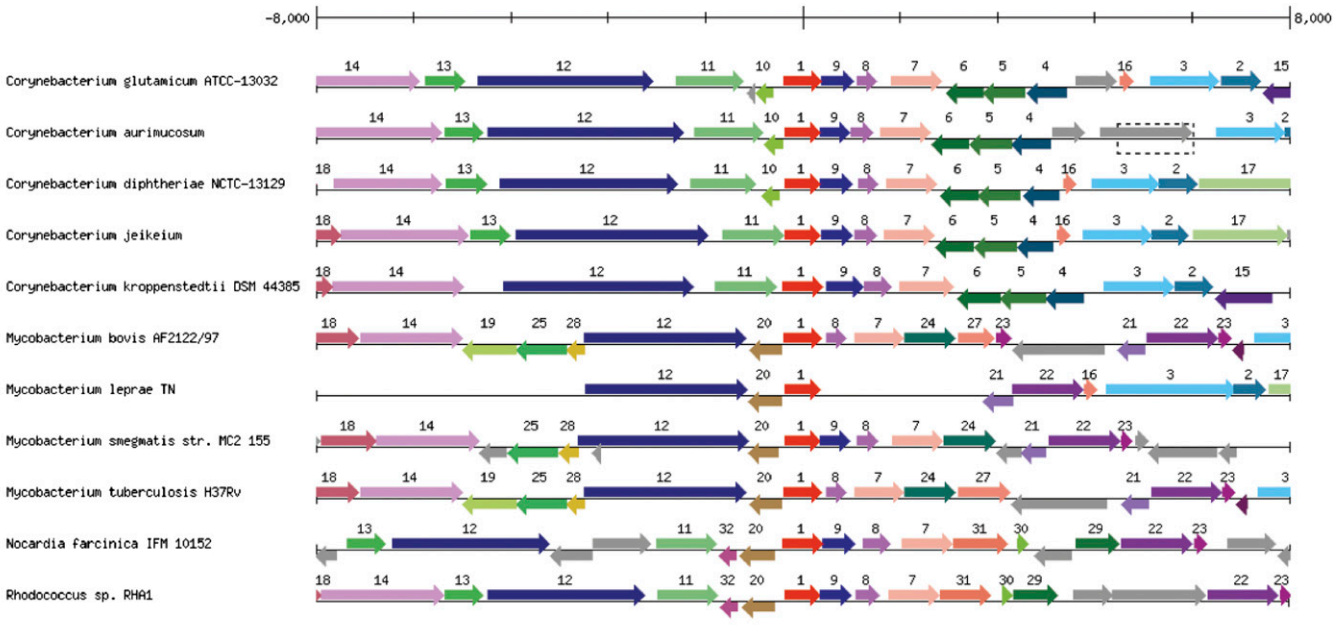

1	CDP-diacylglycerol--glycerol-3-phosphate 3-phosphatidyltransferase	6	Biotin transport energy-coupling factor protein BioN
2	Regulatory protein recX	7	Hypothetical
3	RecA	8	Transcriptional Regulator
4	BioY protein	9	Competence-damage protein cinA
5	Bio M	10	Hypothetical
20	Amino-acid acetyltransferase (EC 2.3.1.1)		

Fig. S4. Generation of pgsA-deficient *Cg*. The gene NCgl1889 encodes pgsA in *Cg* and is the ortholog of Rv2746c in *Corynebacteriales*. Rv2746c is present in a cluster of genes conserved in *Corynebacteriales*, indicating relevant biosynthetic functions. Even in *Mycobacterium leprea* with its decayed genome Rv2746c is retained, as is the divergently transcribed amino acid acetyltransferase gene within all mycobacterial species. Due to the essentiality of Rv2746c in *Mtb* (1), we expected the ortholog NCgl1889 to be essential in *Cg*, too. However, deletion mutants could easily be obtained. Shown are the gene cluster and annotated genes in this region.

1. Sassetti CM, Boyd DH, Rubin EJ (2003) Genes required for mycobacterial growth defined by high density mutagenesis. *Mol Microbiol* 48(1):77–84.

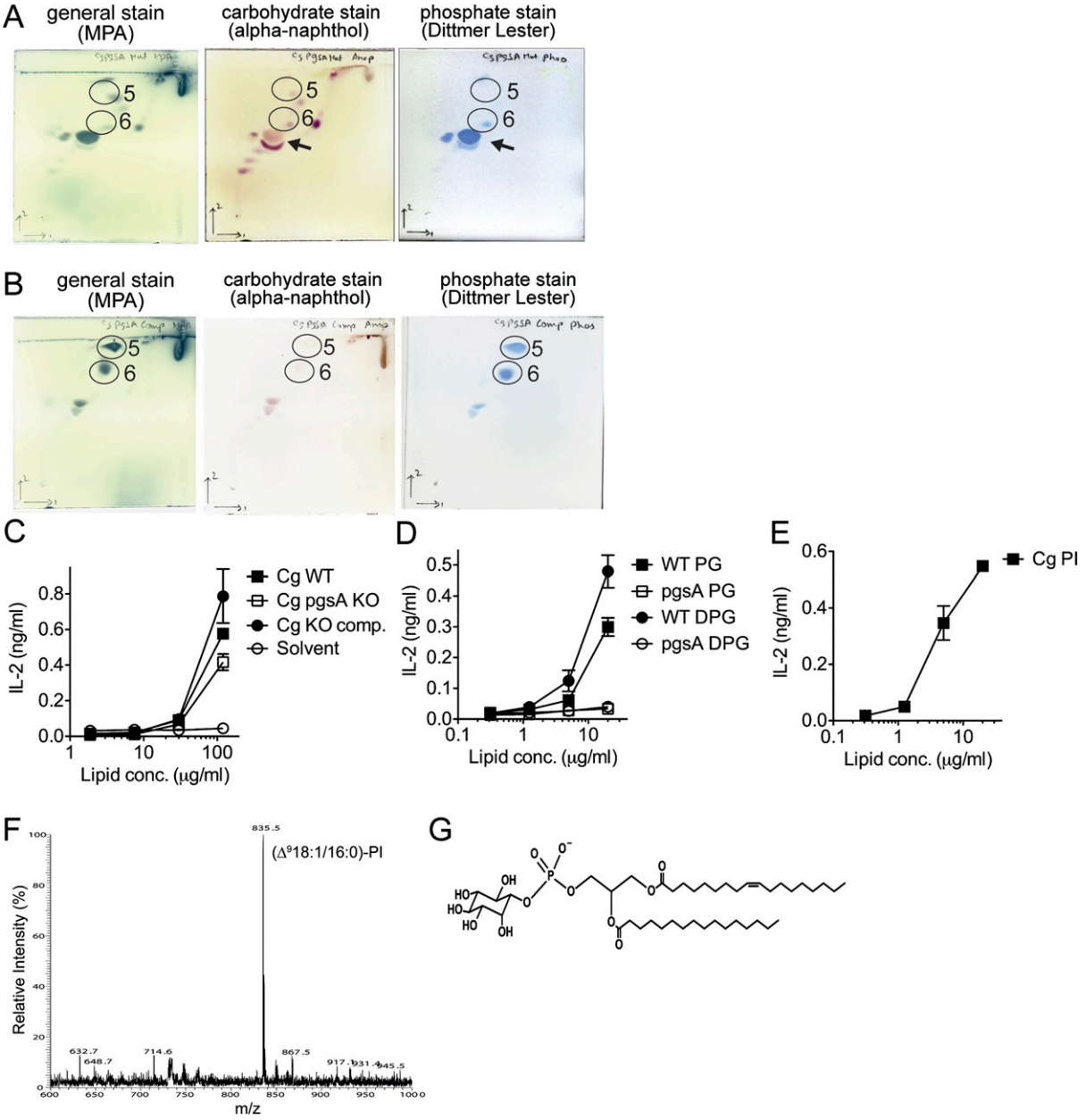

Fig. S5. pgsA-deficient *Cg* lacks production of PG and DPG. Lipid analysis of (*A*) pgsA-deficient *Cg* by 2D-TLC revealed loss of production of PG (p6) and DPG (p5), and increased production of PI (arrow); staining with MPA (left), α-naphtol (middle) and Dittmer Lester reagent (right) are shown. (*B*) pgsA-complemented/pgsA- *Cg* showed a lipid profile similar to WT *Cg* (see Fig. S3B). (*C*) Polar lipids isolated from WT, pgsA-deficient, or pgsA-complemented/pgsA- *Cg* bacteria were added to 14S.10/RAW.CD1d cell cocultures. (*D*) 14S.10 cells were stimulated by PG and DPG from WT *Cg*, but not by lipids isolated from the corresponding locations from pgsA-deficient *Cg*. (*E*) PI from pgsA-deficient *Cg* stimulated 14S.10 cells. (*F*) MS data and (*G*) structure of *Cg* PI. Data are representative of two independent experiments.

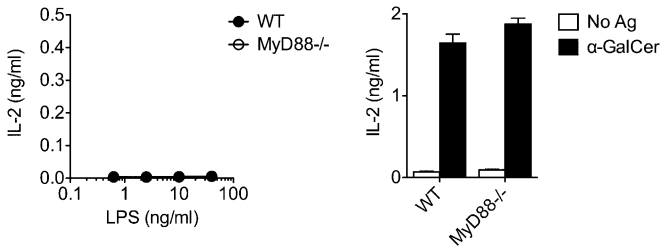

Fig. S6. iNKT hybridomas are not cytokine responsive. The DN32 iNKT hybridoma was stimulated with LPS (*Left*) or α-GalCer (*Right*) in the presence of WT or MyD88$^{-/-}$ BMDCs.